Vision Research 49 (2009) 1681–1692

Contents lists available at ScienceDirect

Vision Research

journal homepage: www.elsevier.com/locate/visres

Interocular transfer of orientation-specific fMRI adaptation reveals amblyopia-related deficits in humans

Alina Jurcoane [a,b,c,d,e], Bhaskar Choubey [a,b,f], Donka Mitsieva [a,b], Lars Muckli [a,c,g,1,*], Ruxandra Sireteanu [a,b,c,h,1,†]

[a] Department of Neurophysiology, Max-Planck-Institute for Brain Research, Frankfurt am Main, Germany
[b] Department of Biological Psychology, Institute for Psychology, Goethe-University, Frankfurt am Main, Germany
[c] Brain Imaging Center, Frankfurt am Main, Germany
[d] Centre for Research on Individual Development and Adaptive Education (IDeA), Frankfurt am Main, Germany
[e] Institute of Neuroradiology, Goethe University, Frankfurt am Main, Germany
[f] Microelectronics Circuits and Analog Devices Group, Department of Engineering Sciences, University of Oxford, United Kingdom
[g] Center for Cognitive Neuroimaging, Department of Psychology, University of Glasgow, United Kingdom
[h] Department of Biomedical Engineering, College of Engineering, Boston University, Boston, Massachusetts, USA

ARTICLE INFO

Article history:
Received 8 August 2008
Received in revised form 3 April 2009

Keywords:
fMRI adaptation
Interocular transfer
Extrastriate visual cortex
Amblyopia

ABSTRACT

We devised an experimental strategy for assessing the cortical cross-talk between ocular subsystems. For this purpose we measured the interocular transfer of adaptation (IOTA) at different levels in the human brain, using orientation-selective fMRI adaptation. We tested 10 normally sighted and 10 stereoblind or stereodeficient amblyopic observers by adapting *monocularly* to phase-reversing, oblique sinusoidal gratings. Following *monocular* adaptation, cortical activations evoked by the same (*monoptic*) or the other eye (*interocular*) were measured for the same and for the orthogonal orientation in a two by two factorial design. In both experimental groups, we obtained significant orientation-selective *monocular* adaptation in area V1 and in extrastriate regions on the dorsal and ventral visual pathways. In the normally-sighted subjects we found in addition interocular adaptation in V1 and extrastriate visual areas. This interocular adaptation indicates that fMRI adaptation transfers from the adapted ocular subsystem to the non-adapted ocular subsystem, and thus provides a measure of binocular interaction in normally-sighted subjects. In the amblyopic subjects, no *interocular* adaptation was seen at any of the investigated cortical levels, regardless of which eye was adapted. We suggest that the abnormal pattern of interocular transfer of fMRI adaptation is related to the disturbed integration of binocular signals in amblyopia.

1. Introduction

Repetitive presentation of a visual stimulus results in decrease of the neural activity evoked by this stimulus (Weigelt, Muckli & Kohler, 2008). This decrease, known as adaptation, can be selective for the orientation and spatial frequency of the adapting stimulus (cf. Blakemore & Campbell, 1969). Monocular adaptation to a grating stimulus can be transferred to the non-adapted eye (cf. Blakemore & Campbell, 1969; Fiorentini, Sireteanu, & Spinelli, 1976; Wolfe & Blake, 1985). This interocular transfer of grating adaptation is believed to be mediated by binocularly driven neurons in the primary visual cortex; indeed, neurons in area 17 of the cat show pattern-selective adaptation, which also transfers to the unadapted eye (Maffei, Fiorentini, & Bisti, 1973; Movshon & Lennie, 1979).

Humans with amblyopia, a condition related to early misalignment of the visual axes (strabismus) or to a refractive imbalance between the two eyes (anisometropia), have been reported to show reduced interocular transfer of pattern adaptation (cf. Blake, 1982; Hohmann & Creutzfeldt, 1975; Mitchell & Ware, 1974; Movshon, Chambers, & Blakemore, 1972; Sireteanu, Fronius, & Singer, 1981; Wade, 1976; Ware & Mitchell, 1974). This reduction was suggested to be related to the loss of binocular neurons in the primary visual cortex, known to occur as a result of an early strabismus or visual deprivation (cf. Hubel, Wiesel, & LeVay, 1977; Kiorpes, Kiper, O'Keefe, Cavanaugh & Movshon, 1998; Kiorpes & McKee, 1999). However, several studies have shown that the interocular transfer of pattern adaptation is not always directly related to the residual stereopsis of an individual subject (cf. Hess, 1978; Maraini & Porta, 1978; McColl & Mitchell, 1998; Mohn & van Hof-van Duin, 1983).

* Corresponding author. Address: Center for Cognitive Neuroimaging, Department of Psychology, University of Glasgow, 58 Hillhead Street, Glasgow G12 8QB, United Kingdom.
E-mail address: l.muckli@psy.gla.ac.uk (L. Muckli).
[1] These two authors have contributed equally to the work.
[†] Deceased.

0042-6989/$ - see front matter Crown Copyright © 2009 Published by Elsevier Ltd. All rights reserved.
doi:10.1016/j.visres.2009.04.009

In the present study, we attempted to address the neural mechanisms underlying these extensively investigated psychophysical phenomena. We developed an experimental strategy using functional Magnetic Resonance Imaging (fMRI) for determining the cortical integration of signals coming from the different eyes. We combined the paradigms of fMRI adaptation (fMRIa) and interocular transfer (IOT) of adaptation obtained after *dichoptic* visual stimulation. The fMRIa method is based on the reduction of the fMRI signal during repeated presentation of identical stimuli (Grill-Spector, Henson, & Martin, 2006; Grill-Spector & Malach, 2001; Kourtzi & Kanwisher, 2001; Weigelt et al., 2008). Orientation-selective fMRI adaptation was described in area V1 (Fang, Murray, Kersten, & He, 2005; Krekelberg, Boynton, & van Wezel, 2006; Larsson, Landy, & Heeger, 2006) and at higher levels on the ventral visual pathway of the human brain (Boynton & Finney, 2003; Krekelberg et al., 2006).

Animal studies suggested that integration of signals coming from the two eyes is more complete in higher-order cortical regions than in area V1 (cats: Sireteanu, 1991; Sireteanu & Best, 1992; von Grünau, 1982; macaque monkeys: Movshon & Newsome, 1996; Shipp & Zeki, 1989). The effects of an early deprivation or strabismus seem to be more profound in higher-order extrastriate regions than in the primary visual cortex (Sireteanu, 1991; Sireteanu & Best, 1992; von Grünau, 1982). Additionally, regions on the ventral visual pathway seem to be more deeply affected than those on the dorsal visual pathway (Schröder, Fries, Roelfsema, Singer, & Engel, 2002). Previous functional imaging experiments are consistent with these findings, by showing that, in humans with strabismic or anisometropic amblyopia, transmission of activity from the amblyopic eye is increasingly impaired while it is relayed towards higher processing levels on the ventral stream (Lerner et al., 2003; Muckli et al., 2006).

Our pilot study, in which we applied this method to test the interocular transfer of fMRI adaptation in two normally-sighted observers and one stereodeficient subject with alternating fixation, yielded encouraging results: we found significant *monoptic* and *dichoptic* fMRI adaptation in area V1 and the extrastriate cortex of the normally-sighted observers, but no *dichoptic* adaptation in the extrastriate cortex of the stereodeficient observer (Jurcoane, Choubey, Muckli, & Sireteanu, 2007). However, it remained unclear whether these were just isolated findings and if the method can be applied to a large population of subjects.

In the present study we applied this method on a larger population of subjects. We tested the effect of *monocular* adaptation to a high-contrast sinusoidal grating on the BOLD activation evoked by a low-contrast grating through the same eye (*monoptic* fMRI adaptation), or the other, unadapted eye (*dichoptic* fMRI adaptation). In a first experiment we tested normally-sighted subjects, while in a second experiment we investigated subjects with amblyopia. In both experiments, we concentrated our analysis on three regions in the brain: the primary visual cortex (area V1) and extrastriate cortical regions on the ventral (EXV) or the dorsal visual pathway (EXD). Parts of the results of this study were reported in abstract form (Jurcoane, Mitsieva, Choubey, Muckli, & Sireteanu, 2008).

2. Materials and methods

2.1. Participants

The participants of this study were volunteers recruited through announcements in the Frankfurt University and in other locations in the Frankfurt area. Exclusion criteria for the subjects were: neurological or psychiatric disorders; current medication; ocular abnormalities; metal parts in the body and claustrophobia.

Prior to the scanning experiments, the subjects were tested with a battery of orthoptic tests, including several stereotests (Lang, TNO and Titmus tests); visual acuity for near and far (Snellen acuity with logMAR spacings, assessed with a C-test); angle of strabismus, assessed with a prism and cover test; pattern of fixation, assessed with the aid of a visuscope; pattern of correspondence, assessed with a Maddox cross and a light and dark red filter. All measurements were performed by professional orthoptists. All normally-sighted subjects had full stereovision and normal or corrected-to-normal vision in each eye. To be classified as amblyopic, the subjects had to show a difference of at least two lines Snellen acuity for single optotypes and no measurable stereopsis with the Lang, TNO and Titmus tests, with the exception of the fly in the Titmus test (corresponding to about 3.500″ stereovision). The orthoptic data of the amblyopic subjects are shown in Table 1.

The experiments were conducted with the written informed consent of each subject, the safety guidelines for MRI research and in compliance with the tenets of the Declaration of Helsinki. The study had been approved by the Ethics Committee of the Frankfurt University. All subjects were naïve to the purpose of the experiments.

2.2. Visual stimuli

The stimuli were generated with an in-house software using DirectX libraries and were presented *dichoptically* on a digital dual-display video system (Resonance Technology, Northridge, California) at a resolution of 800 × 600 pixels subtending 30° horizontal field of view (for a review of dichoptical stimulus presentation, see Choubey, Jurcoane, Muckli & Sireteanu, 2009).

As adapting patterns, we used high-contrast (80%), obliquely oriented sinusoidal gratings alternating in phase, with an alternation rate of 2 Hz. As test stimuli, we used sinusoidal gratings of the same spatial frequency, but with a lower contrast (20%). We used orientations of 45° and 135°, since, even though producing less activation at the level of the primary visual cortex than the cardinal orientations (0° and 90°), they are known to elicit similar activations when compared to each other (Furmanski & Engel, 2000), and also to avoid a horizontal bias (Hansen & Essock, 2004; Sireteanu & Best, 1992). Phase-reversal was used in order to avoid retinal adaptation. Our choice of a relatively low spatial frequency (1.5 c/deg) ensured that the stimuli were within the acuity limits of all subjects. The stimuli had a diameter of 5°, with a central sparing of 1.5°. They were presented on a gray background with the same mean luminance as the test stimuli. Psychophysical tests performed outside of the scanner ensured that these stimuli produced consistent adaptation effects in normally-sighted observers.

To ensure that the subjects fixated the center of the stimulus and to divert their attention away from the stimuli, we used an attention-control task in which the subjects had to indicate through button press the occurrence of a number within a rapid serial presentation of randomly generated alphanumeric characters. Such a task is useful because spatial attention can strongly modulate the neuronal responses to visual stimuli measured with fMRI (Somers, Dale, Seiffert, & Tootell, 1999; Murray, 2008; Simola, Stenbacka & Vanni, 2009).

2.3. Experiment timing

Psychophysical studies showed that adaptation to high-contrast gratings for periods lasting from several tens of seconds to minutes or tens of minutes are necessary for obtaining stable threshold elevation for a subsequently viewed low-contrast grating (cf. Blakemore & Campbell, 1969; Fiorentini et al., 1976). Long adaptation

Table 1
Orthoptic data of the amblyopic subjects. Abbreviations: VD: vertical deviation, +: esotropia, −: exotropia, *: non-dominant eye, visus cc: visual acuity tested with optimal refractive correction, RX: refraction.

Subject	Gender, age	Eye	Refraction	Visus c.c. (near)	Fixation	Strabismus (sim. cover test)	Stereo (TNO)	History
VH	Female, 22 yr	RE*	0.00 − 0.50/180°	1.25	Central	Far + 2½° + VD3°	∅	Family history, congenital squint, two surgeries (1 and 3 yr), first RX at 1 yr
		LE	+0.50 − 0.50/17°	0.90	Central, unsteady	Near + 3½° + VD3°		
KP	Female, 24 yr	RE*	Plano	1.00	Central	Far − 10°	∅	Early squint, first RX in childhood, alternating occlusion from 3 to 8 yr, surgery at 6 yr (both eyes), two surgeries at 17 yr (RE) – diplopia
		LE*	+0.75	0.80	Parafovea	Near − 6° − VD1°		
US	Female, 47 yr	RE*	−7.00 − 0.75/2°	0.90	Central	Far − ½° + VD1½°	∅	Family history; anisometropia; squint detected at 1–2 yr; first RX at 3 yr; occlusion therapy; three surgeries (8–9 yr)
		LE*	−3.25	0.70	Central, unsteady	Near − 4½°		
CB	Female, 31 yr	RE*	−2.50	0.70	Central, unsteady	Far + 2°	∅	Family history; congenital strabismus, first RX at 1½ yr, occlusion therapy, RE crowding
		LE*	−3.75	1.25	Central	Near + 3.5°	Titmus fly	
KK	Female, 22 yr	RE*	+3.75	0.70	Central	Far + 1°	∅	Microstrabismus, occlusion therapy between 5 and 7 yr, first RX at 7 yr
		LE*	+4.00	1.25	Central	Near + 2°	Titmus fly	
KL	Female, 25 yr	RE*	+1.00 − 0.75/114°	0.70	Central, unsteady	Far + 1° + VD1.5°	∅	Premature birth; congenital strabismus; anisometropia; first RX at 3 yr; occlusion therapy from age 3 to 7, surgery at 10 yr; RE crowding
		LE*	−3.00 − 0.50/61°	1.00	Central	Near + 1° + VD1.5°	Titmus fly	
CS	Female, 36 yr	RE*	+2.75 − 1.00/84°	0.50	Central	Far + 3° − VD2°	∅	Early squint, anisometropia; occlusion from age 2 to 6, first RX at age 2, two surgeries (RE at 6, both eyes at 33 yr)
		LE*	+0.75 − 0.50/3°	1.00	Central, unsteady	Near + 3° − VD2°		
HM	Male, 58 yr	RE*	+5.50 − 3.25/14°	0.40	Central, unsteady	Far + VD8°	∅	Squint since birth, anisometropia; occlusion therapy and RX in childhood, three surgeries (both eyes) at 8 and 13 yr
		LE	+2.25 − 1.75/0°	1.00	Central, unsteady	Near + VD8°		
KF	Female, 43 yr	RE*	−1.50 − 0.25/60°	1.00	Central	Far − 19°	∅	First RX at 3 yr, anisometropia; occlusion therapy from 3 to 7 yr; diplopia
		LE*	0.00 − 0.50/0°	0.40	Central	Near − 17.5°		
SS	Female, 43 yr	RE*	+0.50 − 0.50/90°	0.32	Parafovea	Far + 3°	∅	Congenital esotropia; two surgeries RE at ca. 2–3 yr; occlusion therapy at 4–6 yr; glasses from 6 to 11 yr; crossed dominance, RE crowding
		LE	+0.25 − 0.50/120°	1.25	Central	Near + 3°	Titmus fly	

periods are not practicable in the fMRI environment, due to the limited amount of time allocated for an experiment. Selective adaptation experiments involving fMRI have so far used short-lasting adaptation periods in the millisecond range (Krekelberg et al., 2006; Larsson et al., 2006). Since in our pilot experiments adapting times in the millisecond range did not elicit consistent adaptation in the primary visual cortex, we adopted a procedure introduced by Fang and colleagues (Fang et al., 2005) for a pre-adaptation period of 150 s before each session and "topping-up" or refresh adaptations of an intermediate duration (3.5 s) before each test trial (see Fig. 1). Our pilot experiment (Jurcoane et al., 2007) showed that this timing was sufficient to evoke consistent effects of adaptation.

Each fMRI session comprised of three experimental runs (see Section 2.4). Five experimental conditions were used (see Section 2.4) and each of them was presented 25 times per functional run. A set of three dummy conditions were introduced at the beginning of each run to ensure consistency in the back-history of each condition, thereby leading to a total of 128 trials for each run. The succession of the events was designed to ensure an equal number of occurrences for each of the five conditions and a unique 2-back history for each trial through a pseudo-randomized sequence of these conditions (Alink, Singer & Muckli, 2008). The whole experiment lasted 1 h and 10 min of effective scanning and contained three functional runs of experiment, one anatomical scan and one additional functional scan for mapping of the visual areas. Each of the three experimental runs used different randomisation sequences.

To eliminate any bias resulting from stimulation of one eye more than the other, we alternated the use of dominant/non-dominant eye stimulation within the three experimental runs of each subject and counterbalanced the use of each eye within subjects. Unlike in subjects with amblyopia, in normally-sighted persons ocular dominance is less obvious (Seijas et al., 2007) and might vary, according to the used dominance test or the testing distance (own unpublished observations and Rice, Leske, Smestad, & Holmes, 2008). Therefore, for the normally-sighted group we coun-

Fig. 1. (A) Stimuli used during the experiments – adapting grating (most left), testing gratings (center) and fixation (most right). (B) Summary of the experimental conditions and timing. RE = right eye, LE = left eye.

terbalanced the right with the left eye and for the amblyopic group, we counterbalanced the dominant and the non-dominant eye.

2.4. Testing conditions

In both experiments, the observers were tested under five experimental conditions: *monocular* adapted (MonA), *monocular* non-adapted-control (MonC), interocular adapted (IOTA), interocular non-adapted-control (IOTC) and gray background as baseline (Fix). Details of the timing protocol are shown in Fig. 1A. We compared in the first step MonA with MonC and in a second step IOTA with IOTC. The first comparison was the verification that adaptation was present at a specific cortical level, while the second comparison was the proof of the existence of interocular transfer at this level (for details, see Fig. 1).

2.5. Imaging parameters, data analysis

We used a 3T Siemens MRI Allegra scanner, with a rapid event-related fMRI protocol in which the conditions were presented in a pseudo-randomized sequence. The experiments were conducted with a one channel bird-cage head-coil and head position was fixed by means of lateral foam cushions. Anatomical images were acquired using a T1-weighted 3-D magnetization prepared rapid acquisition gradient echo sequence (MP RAGE) in the same session as the functional measurements. Each anatomical scan lasted 8 min and yielded 160 sagittal slices of 1 mm^3 voxel resolution (TR = 2300 ms, TE = 3.93 ms, FA = 12°, 256 × 256 acquisition matrix). Functional images were acquired using a multislice $T2^*$-weighted echo-planar imaging (EPI) sequence (TR = 1000 ms, TE = 28 ms, FA = 60°, number of slices = 18, slice thickness = 3.3 mm, with a 64 × 64 acquisition matrix and a 210 × 210 mm rectangular field of view, providing a voxel resolution of 3.3 mm). For each dynamic scan, 938 measurements (MRI volumes) were acquired, leading to a total scanning time of 16 min per experimental run. Three experimental runs were performed in each session.

Anatomical data from individual participants were first corrected for intensity inhomogeneities (iterative procedure of bias field removal) and subsequently transformed into the stereotaxic space of Talairach and Tournoux (1988). This transformation was accomplished by manually identifying the anterior and posterior commissures, the highest point in the midsagittal plane and the bounding edges of the brain. These points were used to linearly orient and scale the sagittal images into Talairach space using trilinear interpolation. Further, we applied an automatic tissue segmentation technique followed by cortex inflation procedures. Functional data were pre-processed and analyzed using the Brain Voyager QX software package (BrainInnovation, Maastricht, The Netherlands) and additional statistical tests were performed using SPSS 13.0 (SPSS, Inc., Chicago, IL).

During pre-processing, functional data underwent slice scan-time correction, 3-D motion correction, linear trend removal and high-pass temporal filtering at 0.01 Hz. The preprocessed data were co registered with the anatomical data and functional data statistics was superimposed on the high resolution anatomically reconstructed cortex. Statistical analysis was done using a fixed effect deconvolution general linear model (GLM) of 20 time points for each condition using the baseline condition Fix as reference. During the GLM computation we applied a percent signal change correction that insured that the time course of a voxel or a region-of-interest is normalized in such a way that the mean signal value is transformed to a value of 100 with the individual values fluctuating around the mean as percent signal deviations. Thus, the reported signal change beta weights directly provide an estimate of the actual percent signal change (Weigelt, Kourtzi, Kohler, Singer, & Muckli, 2007). Impulse response functions plotted for the modeled response (beta weights) at 1–15 s after onset of the stimulus.

Considering the temporal profile of the BOLD response (it takes 4–6 s for a signal to reach its peak after the stimulus onset – see Boynton, Engel, Glover, & Heeger, 1996) and given the timing of our experimental conditions (the first 3.75 s of stimulus presentation were identical for all conditions), we expected to record noticeable differences related to fMRI adaptation between our conditions after 7–8 s from beginning of the presentation of each condition. Therefore, we analyzed differences at 8–9–10 s after the beginning of stimulus presentation and differences were deemed significant for a threshold level of $p < 0.05$. As a control, we also analyzed the data at 7–8–9–10 s after onset of stimulus presentation; since there were no differences in the outcome of the analysis, only data based on differences at 8–9–10 s shall be presented here.

2.6. Region of interest selection

We based the selection of regions of interest (ROI) on the hemodynamic response peaks: since the highest hemodynamic response for each condition was reached 6–7 s after stimulus onset, we chose those areas that had a coherent, positive response around these time-points, namely 5–6–7–8 s after stimulus onset. Based on these peaks, we defined the three regions of interest using anatomical landmarks. In each individual subjects we used cortical reconstructions to identify patches of highest activation along the calcarine sulcus as V1, while activations outside V1 were identified as EXD when they were situated towards the dorso-parietal regions and EXV when they were situated ventral to V1, towards the temporal regions (for examples, see Fig. 2).

To make sure that this strategy for region selection based on anatomical landmarks did not differ from retinotopic mapping, we compared the results of anatomically-driven region selection with those of a retinotopic mapping obtained using a rotating checkerboard wedge (polar mapping, for details, see Goebel, Khorram-Sefat, Muckli, Hacker, & Singer, 1998; Goebel, Muckli, Zanella, Singer, & Stoerig, 2001; Meienbrock, Naumer, Doehrmann, Singer, & Muckli, 2007; Muckli, Kohler, Kriegeskorte, & Singer, 2005; Muckli et al., 2006; Weigelt et al., 2007). The two methods show a very high consistency: the V1 region defined anatomically corresponded in all cases to the retinotopic area V1 (see black markings and notations in Fig. 2).

As revealed by the retinotopic maps, our EXV included mostly areas V2v and V3v, while our EXD included parts of V2d and V3d. The pattern of activation based on retinotopic mapping was strikingly respecting the anatomical landmarks; in most subjects V1 activation appeared as a stand-alone patch of activation (see Fig. 2). Our procedure is also consistent with the findings of Vanni, Henriksson and James (2005) who used multifocal retinotopic mapping and confirmed high signal responses for V1, confirming that V1 can be separated with using high signal response thresholds.

3. Results

3.1. Experiment 1: dichoptic fMRI adaptation in normally-sighted observers

The first experiment was conducted with a group of ten subjects with intact stereovision (seven females and three males; mean age 25.0 years). We tested the effect of adapting one eye to a high-contrast sinusoidal grating on the cortical activity evoked by stimulation with a low-contrast grating, either through the same eye (*monoptic* adaptation) or through the other, non-adapted eye (*dichoptic* adaptation).

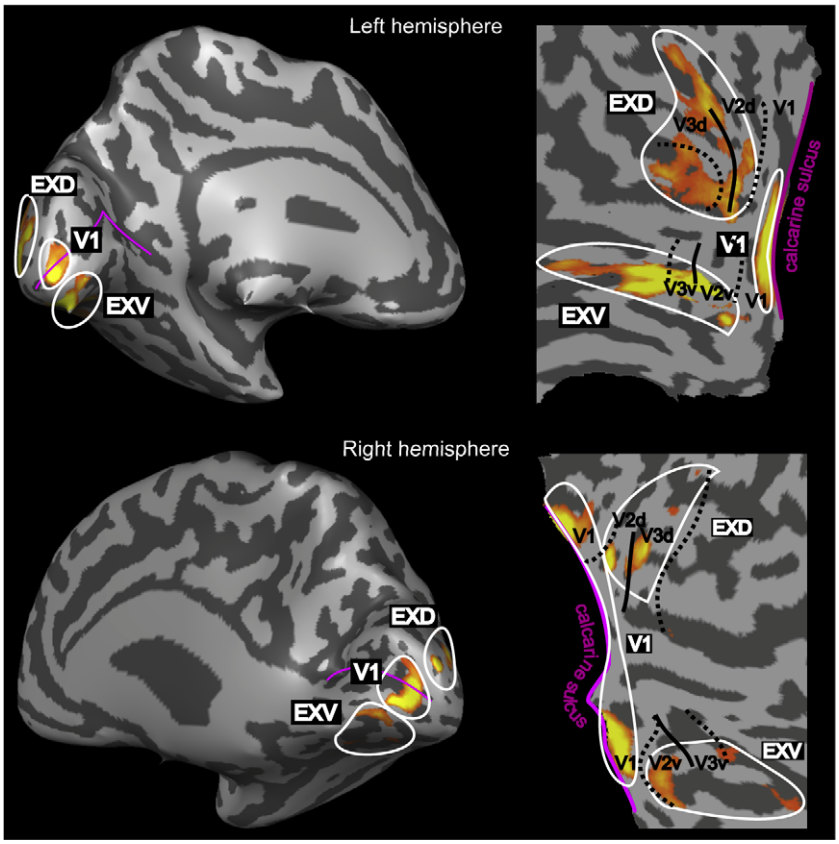

Fig. 2. Examples for the selection of the regions of interest (ROIs). Statistical maps superimposed on inflated (left panel) and flattened (right panel) surfaces of the reconstructed cortex of one normally-sighted subject (left hemisphere, upper panel) and one amblyopic subject (right hemisphere, lower panel). Based on anatomical landmarks (calcarine sulcus – pink line) we selected three regions of interest (white marks): the striate cortex (V1), the extrastriate ventral (EXV) and extrastriate dorsal (EXD) cortex. For comparison, corresponding retinotopically mapped locations are marked with black.

3.1.1. Data averaged over eyes

The results of this experiment, averaged over all subjects and both eyes, are shown in Fig. 3A. We found significant *monocular* activations at all investigated cortical levels, peaking at about 6 s after stimulus onset (dark green[2] curves in Fig. 3A). At all levels, cortical activation was significantly reduced after adaptation of the same eye (light green curves in Fig. 3A). Adaptation was more pronounced in the extrastriate regions EXD and EXV ($p < 0.000001$) than in the striate region V1 ($p < 0.004$) indicating a higher reliability of the effects of adaptation in higher cortical areas.

At all cortical levels, we also found highly significant reductions of cortical activation after *dichoptic* adaptation (compare red and pink curves in Fig. 3A). Similar to its *monocular* counterpart, the *dichoptic* adaptation was more pronounced in the extrastriate regions ($p < 0.000003$ in both EXD and EXV) than in V1 ($p < 0.03$) (compare upper with middle and lower panels in Fig. 3A).

Dichoptic adaptation effects were always smaller than those of *monoptic* adaptation. When calculating the strength of the *dichoptic* adaptation as a percentage of the *monoptic* adaptation, we obtained 63% in area V1, 57% in area EXD and 58% in EXV.

3.1.2. Separate eye analysis

We also analyzed the data of the normally-sighted subjects separately for adapted eyes and the data were separated on a right/left eye basis. The results are shown in Fig. 4A and B.

The results were similar to the results of the averaged-eyes analysis in the extrastriate regions EXV and EXD (significant *monocular* as well as *dichoptic* adaptation). Area V1, however, failed to exhibit significant *dichoptic* adaptation for the left eye and significant *monocular* adaptation for the right eye.

3.2. Experiment 2: dichoptic fMRI adaptation in amblyopic subjects

The results of this experiment were based on data from ten amblyopic observers with differing degrees of amblyopia (nine females and one male; mean age 35.1 years). All subjects were strabismic; five of them were also anisometropic. Nine of the ten subjects had undergone occlusion therapy during childhood. Of these, seven also underwent surgeries at different ages (see Table 1).

3.2.1. Data averaged over eyes

The results are shown in Fig. 3B. At all tested cortical locations, activation peaked at around 6–7 s after stimulus onset. First we compared the overall level of activation response in V1, EXD and EXV of the group with amblyopia to the normally-sighted control group: The activation peak is lower for the amblyopic group in V1 and EXD ($p < 0.05$) but only slightly reduced in EXV ($p > 0.05$) (compare the height of the curves in Fig. 3B with the peak BOLD response (beta values) of the normally-sighted group represented by a reference dotted line). The averaged signal for the end of the response (8–10 s after onset), given in the beta-value bar plots (right in Fig. 3A and B), is however not different between the groups.

Adaptation produced different effects on the cortical activity evoked through the same eye (*monoptic* adaptation) than through

[2] For interpretation of color in Fig. 6, the reader is referred to the web version of this article.

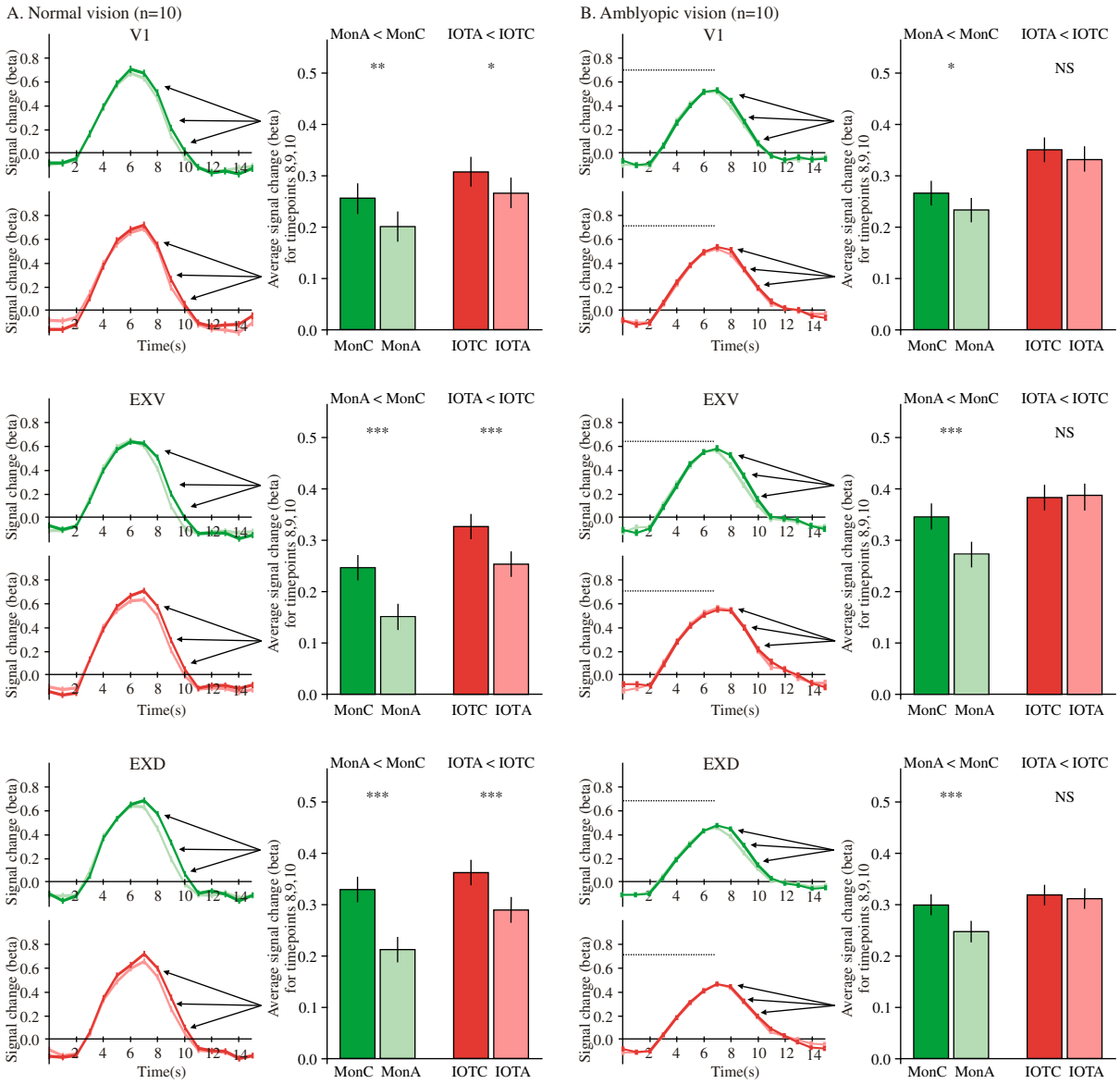

Fig. 3. Effects of fMRI adaptation. Comparison of monoptic and dichoptic adaptation. (A) Normally-sighted observers and (B) Amblyopic observers. For both (A) and (B): left panels – time course of the BOLD signal (beta values); right panels – columns representing the averaged activity for the relevant time points. Results are shown for area V1 (top), extrastriate ventral regions (EXV) (middle) and extrastriate dorsal regions (EXD) (bottom). Green symbols indicate *monoptic* adaptation, red symbols *dichoptic* adaptation. Dark curves: control activation (response to unadapted orientation); light curves: adapted activation (response to adapted orientation). In all cases, the results were pooled over both eyes. In B the horizontal dotted line represents the peak activation level in the normally-sighted group in the same cortical region and for the same conditions. Error bars indicate standard errors of the mean. Stars denoting significance levels represent: $^{*}p < 0.05$, $^{**}p < 0.01$, $^{***}p < 0.001$.

the other eye (*dichoptic* adaptation). A statistically significant decrease of activity after *monoptic* adaptation was seen at all levels. As in the normally-sighted subjects, this decrease of activity was more pronounced in extrastriate regions than in the striate area (V1: $p < 0.04$, EXD: $p < 0.000004$, EXV: $p < 0.00004$; see dark and light green columns in Fig. 3B). No *dichoptic* adaptation was seen, at any of the investigated cortical levels (see red and pink columns in Fig. 3B).

3.2.2. Separate eye analysis

When analyzing separately the effect of adapting the dominant (non-amblyopic) and the non-dominant (amblyopic) eye (see Fig. 4C and D), we found in the extrastriate regions (both dorsal EXD and ventral EXV) a similar pattern as in the averaged-eyes analysis in the same subjects: adaptation of the dominant as well as of the non-dominant eye led to a statistically significant *monoptic* fMRI adaptation and no interocular transfer of this adaptation.

Intriguingly, Area V1 of the amblyopic observers not only failed to show any interocular transfer, but also failed to exhibit *monocular* adaptation through the dominant eye. It is interesting to note that in normally-sighted observers, *monocular* adaptation in Area V1 also failed to reach statistical significance in the right eye (see upper panels in Fig. 4).

3.3. Group comparisons

Single subject data were similar to the group data, in the striate regions but even more pronouncedly in the extrastriate visual areas. Amblyopic subjects showed more variability than the normally sighted in all investigated regions (see Fig. 5).

To evaluate the group differences between the magnitudes of the adaptation, statistical analysis was performed using a repeated-measures analysis of variance (ANOVA) model which included vision status (normal or amblyopic) as one factor and

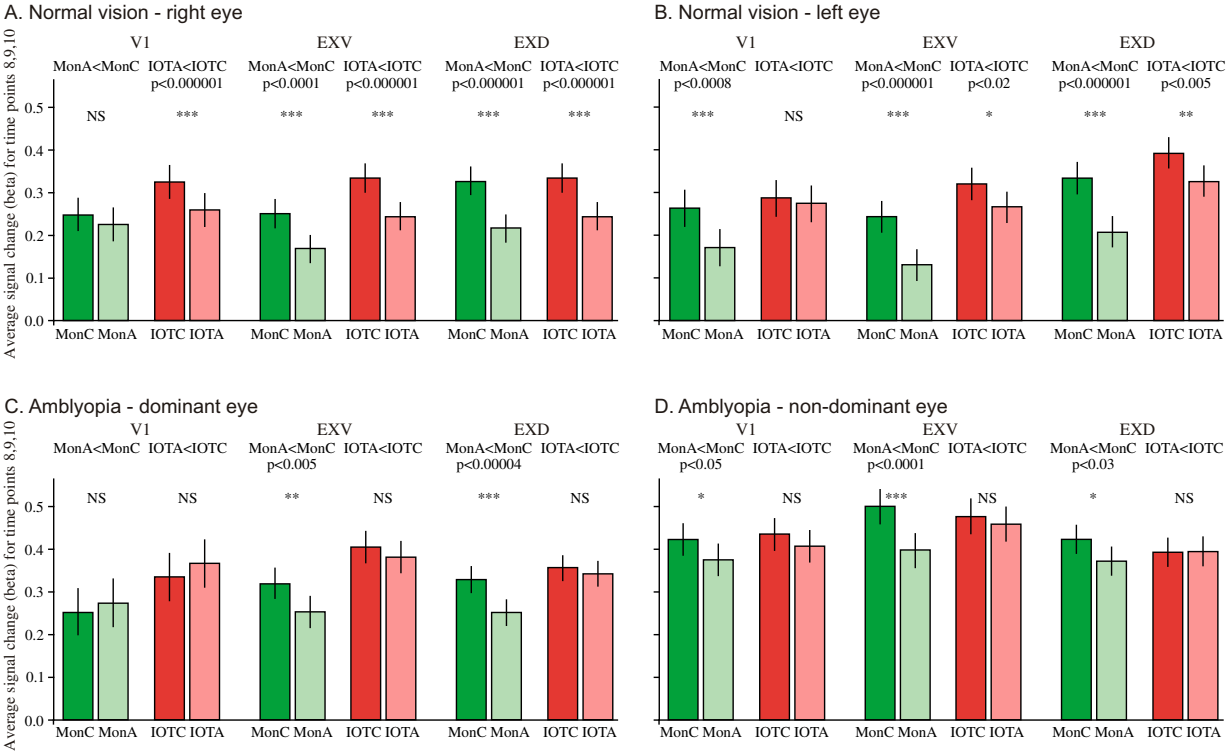

Fig. 4. Separate eye analysis. Upper panel (A and B) – normally-sighted observers; lower panel (C and D) – amblyopic observers. Averaged activity for the relevant time points. Results are shown for area V1, extrastriate ventral regions (EXV) and extrastriate dorsal regions (EXD). Symbols and colors as in Fig. 3.

percent of adaptation (*monocular* or *interocularly transfered*) as another factor. While at the level of V1 there were no detectable differences between the groups, in the extrastriate regions there was marginally less adaptation in amblyopes than in the normally-sighted observers (in region EXV: $F = 4.365$ $p = 0.066$ and in region EXD: $F = 4.667$ $p = 0.059$). At the same time, in the extrastriate regions monocular adaptation was significantly stronger than the transferred, interocular effect (in region EXV: $F = 18.434$ $p = 0.002$ and in region EXD: $F = 6.986$ $p = 0.027$).

The psychophysical data collected during the fMRI experiments (manual reaction times and percent correct responses) showed consistently faster reaction times ($p < 0.003$) for the normally sighted than for the amblyopic group (reaction times 533 ± 94 ms, respectively, 621 ± 129 ms) (Fig. 6A). Additionally, the normally-sighted group performed the task more accurately than the amblyopic group (95 ± 7%, respectively, 90 ± 9.5% correct responses; $p < 0.03$) (Fig. 6B). In relation to stimulus type, more mistakes occurred when the target was concomitant with the oriented gratings than when the target occurred alone on the fixation background. However, there was no significant difference related to which grating was presented (low or high contrast) or to how this grating was presented (monocularly or dichoptically) (Fig. 6C).

4. Discussion

The main goal of this study was to demonstrate interocular transfer of orientation-specific fMRI adaptation. In addition, we aimed to test the reduction of interocular connectivity in amblyopia and to investigate whether fMRI adaptation can be used as a tool for studying binocular interaction at different levels in the human brain.

4.1. Evaluation of the results in normally-sighted observers

We found highly reliable cortical effects of *monocular* orientation-specific effects of fMRI adaptation in individuals with normal vision. In spite of the slightly modified procedure, these results confirm and extend earlier reports in which *binocular* orientation-specific fMRI adaptation was investigated (Boynton & Finney, 2003; Fang et al., 2005; Larsson et al., 2006). As expected from previous studies (Krekelberg et al., 2006), the effects of adaptation in extrastriate areas were higher and more reliable than in area V1.

In addition to *monocular* adaptation, in normally-sighted subjects we also found significant effects of *dichoptic* fMRI adaptation. The presence of dichoptic adaptation suggests that, adaptation of one eye to an oriented grating pattern consistently affects the cortical activity evoked by the other, unadapted eye. We interpret this behavior as a proof of interocular transfer of the *monoptic* adaptation. To our knowledge, our study is the first to report interocular transfer of fMRI adaptation in normally-sighted subjects. *Dichoptic* adaptation was found both in area 17 and at higher levels on the ventral and dorsal extrastriate visual pathway. In area V1, though weak adaptation was measured, the interocular transfer effects were of a similar magnitude as the interocular transfer of grating adaptation determined psychophysically (50–80%; Fiorentini et al., 1976; Mitchell & Ware, 1974; Sireteanu et al., 1981; Ware & Mitchell, 1974; Wolfe & Blake, 1985), thus confirming that the visual cortex of human observers contains a substantial amount of orientation-specific binocular cells. It was somewhat surprising that the amount of interocular transfer in extrastriate areas was not larger than in area V1. Indeed, in macaque monkeys, practically all cells in extrastriate cortical areas on both pathways are binocular (Movshon & Newsome, 1996; Shipp & Zeki, 1989). Psychophysical studies indicate that the different after-effects might be based on the activity of neural populations located in different cortical areas (Hess, Hutchinson, Legdeway, & Mansouri, 2007; McColl & Mitchell, 1998; Mohn & van Hof-van Duin, 1983; Raymond, 1993). Moreover, previous electrophysiological and functional imaging data show that the binocular integration of signals leading to fine stereopsis might be more complete in regions on the ventral than on the dorsal visual pathway (Neri, 2005). Our results in nor-

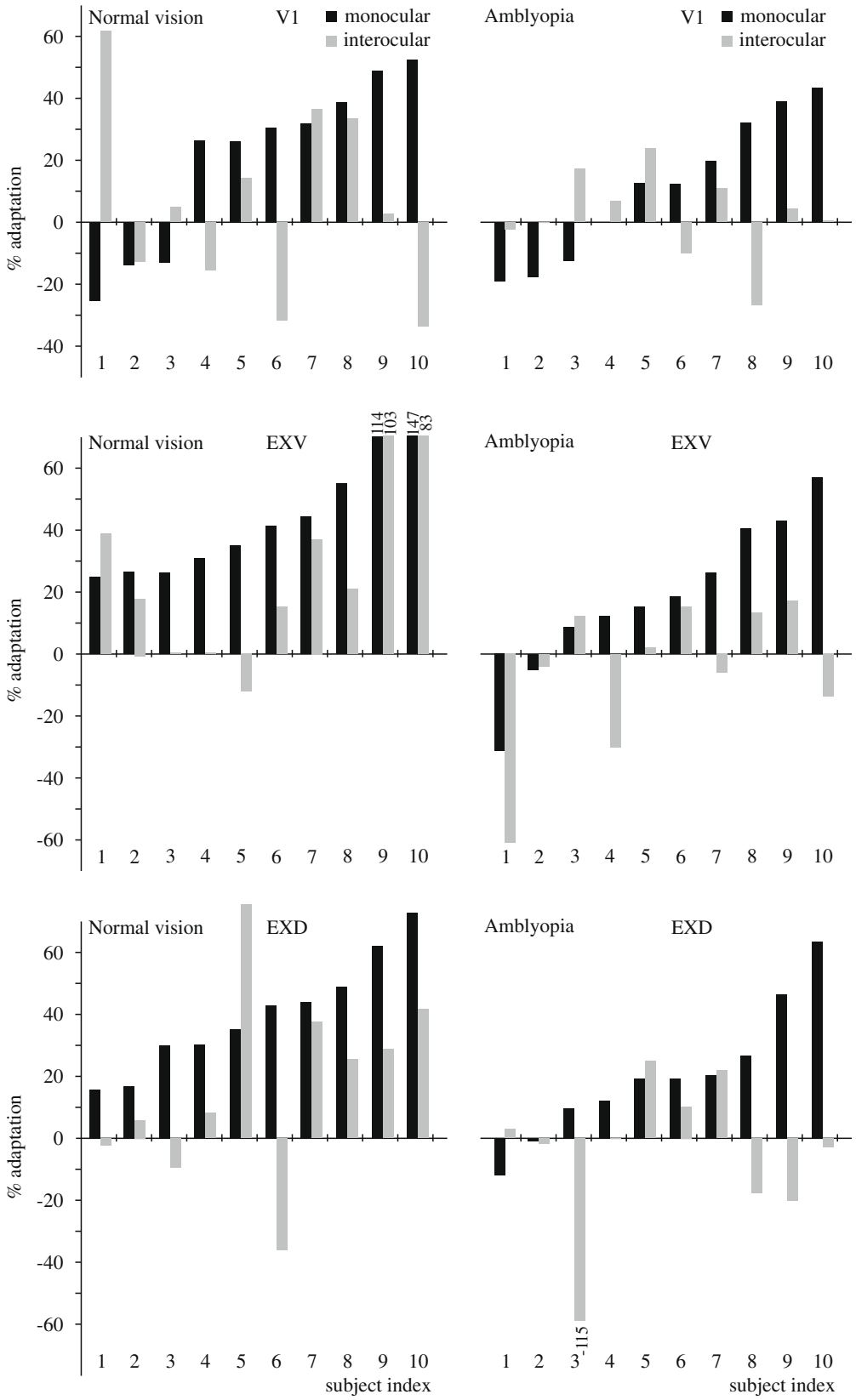

Fig. 5. Single subject data. Percent of monocular (black bars) and interocular (light bars) adaptation for the single subjects. Left panel – normally-sighted group, right panel – amblyopic group. Results are shown for the three regions of interest: the striate cortex (V1) - top row, the extrastriate ventral (EXV) - middle row and the extrastriate dorsal (EXD) cortex - bottom row.

mally-sighted observers, however, do not show such a dichotomy. One possible explanation for this discrepancy might be that our choice of sinusoidal gratings alternating in phase might have limited the analysis to particular classes of cells in these relatively

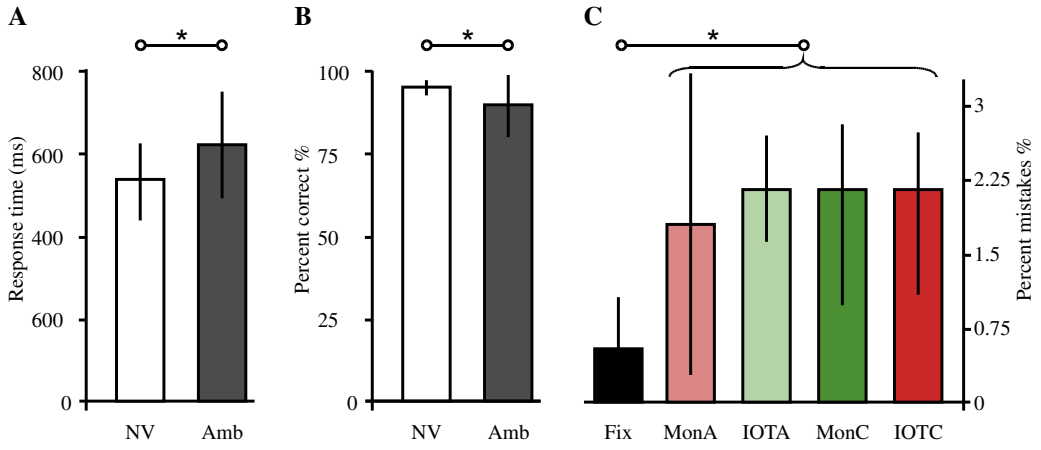

Fig. 6. Behavioural data. Performance for the attention-control task (identifying a number within a rapid serial presentation of alphanumeric characters). Results are shown for the normally sighted (NV) (A, B) and for the amblyopic (Amb) group (A–C). (A) Response times, (B) percent correct responses and (C) percent mistakes in the amblyopic group in relation to the concomitant stimuli (Fix, MonA, MonC, IOTA and IOTC denote the experimental conditions defined in Section 2).

low-level extrastriate visual areas. Even within these areas, some cells might not respond to our stimuli. Our particular pattern of results may be highly dependent on the type of stimuli used. Further studies, using for example other spatial frequencies or more specific visual stimuli, like faces, places, or global motion stimuli, are needed to give full account for pattern of monoptic/dichoptic adaptation, at low-level as well as higher-order visual areas on both the ventral and the dorsal visual pathways.

4.2. Evaluation of the results in amblyopic observers

In contrast to the normally-sighted group, amblyopic subjects with impaired binocular vision, apart for the overall lower levels of cortical activity, showed an abnormal pattern of *dichoptic* fMRI adaptation. They showed significant levels of *monoptic* adaptation, but no *dichoptic* adaptation, at any of the investigated cortical levels and regardless of which eye was adapted. This pattern suggests that the integration of signals coming from the two eyes is impaired in observers with compromised stereopsis. We thus confirmed and extended the results of our pilot study, in which we found good interocular transfer of grating adaptation in both the striate and extrastriate cortex of two normally-sighted observers, but no interocular transfer of adaptation in the extrastriate cortex of one stereoblind observer (Jurcoane et al., 2007).

Our results can not be accounted for by an assumed lack of visibility of the stimuli in the amblyopic group. All gratings were chosen to be well above the contrast threshold and all stimuli (low/high contrast as well as monoptic/dichoptic) produced highly similar fMRI activation. Moreover, by employing a fixation task at the eye that received the grating stimulus, we were able enhance the switch from the dominant to the non-dominant eye (and back) and insure the stimulation of the desired eye. The performance between groups was largely comparable, however, amblyopes had slower response times ($p < 0.003$), which is an indication for more variance across subjects and might account for the reduced peak response in BOLD signal of amblypoes (which is not seen if the BOLD signal is averaged for 8–10 s after onset). Moreover amblyopes performed slightly poorer ($p < 0.03$) on the fixation task than the normally-sighted group which is a common finding reported by several other groups and our own (Hamasaki & Flynn, 1981; Muckli et al., 2006). It is worth noting that in relation to stimulus type, performance was poorer when the target appeared during presentation of the oriented gratings (low/high contrast, monoptic/dichoptic presentation) than when the target occurred alone on the fixation background. These findings can be accounted for by the impaired ability of amblyopes to discriminate targets in noise (Levi, Klein, & Chen, 2008) with noise being in this case the distracting gratings. Another explanation might be the disrupted attentive processing reported in amblyopes (Popple & Levi, 2008), or their deficit in fine motor skills (Webber, Wood, Gole, & Brown, 2008).

4.3. Further findings

Similar patterns of activation were obtained in each group upon in further analysis which investigated the right/left eye or the dominant/non-dominant eye separately. At this in depth analysis, Area V1, however, failed to show significant *monocular* adaptation for the right eye of normally-sighted observers and for the dominant eye of amblyopic observers. We interpret this result as a consequence of the combination of reduced power of the separate eye analysis (only half the dataset is included in this analysis) and of weakness of adaptation in V1. Additionally, as region V1 is obviously smaller than the extrastriate ROIs which include several visual areas, the difference in size and consequently the lower contrast to noise ration might also add to explain the difference in adaptation effects between V1 and extrastriate cortex.

Group comparisons revealed differences only in the extrastriate visual areas but not in V1. We found stronger monocular adaptation compared to the interocular transfer in both groups and less adaptation in amblyopes compared to the normally-sighted subjects. However, we did not find any interaction effect between the groups. Instead, our results seem to point towards a linear combination (addition) of two effects. The order of decreasing adaptation being: normal subjects monocular > amblyopes monocular > normal subjects IOT > amblyopes IOT it follows that IOT in amblyopes around zero could be predicted by the linear summation. It might as well be that our study does not have enough statistical power to decide weather the lack of IOT in amblyopes is caused by a true interaction or just by a linear summation of effects. However, several other studies have found a relation between interocular transfer and stereodeficiency in amblyopia (see discussion on the possible neural mechanisms).

4.4. Possible neural mechanisms

Since both *monocular* and binocular cells are expected to show adaptation in *monocular* trials, whereas only binocular cells are expected to show adaptation effects in *dichoptic* trials, it follows that in normally-sighted observers more than half of the orientation-

specific cells in human area V1 must receive binocular input. This result agrees with data from animal studies: in area V1 of macaque monkeys, the receptive fields of cells in the input layer 4 are non-oriented and *monocular*, while those of the majority of cells in supra- and infragranular layers are orientation-specific and binocular (cf. Hubel & Livingstone, 1987; Hubel et al., 1977; Kiorpes, Kiper, O'Keefe, Cavanaugh, & Movshon, 1998). We therefore suggest that the interocular transfer of grating adaptation might be related to the activity of the orientation-specific, binocular cells in the upper and lower layers in area V1. This hypothesis is further supported by the fact that in amblyopic subjects we did not find any *dichoptic* adaptation and thus no interocular transfer of adaptation in any of the visual areas investigated. Several psychophysical studies showed that the interocular transfer of adaptation after-effects is impaired in subjects with compromised binocular vision (cf. Blake, 1982; Hohmann & Creutzfeldt, 1975; Mitchell & Ware, 1974; Movshon et al., 1972; Sireteanu et al., 1981; Wade, 1976; Ware & Mitchell, 1974).

However, presence of interocular transfer of adaptation was occasionally reported in individuals lacking stereopsis, suggesting a complex relationship between stereopsis and the interocular transfer of the different psychophysical aftereffects (cf. Hess, 1978; Keck & Price, 1982; Maraini & Porta, 1978; McColl & Mitchell, 1998; Mohn & van Hof-van Duin, 1983; McColl, Ziegler & Hess, 2000). For instance, Keck and Price (1982) and Maraini and Porta (1978) found an asymmetric transfer of adaptation, that is, right-left transfer did not equal left–right transfer. Interocular transfer was deeply impaired when the dominant eye was adapted, but much less so when the non-dominant eye was adapted. We could not observe such an asymmetry but this might mean that individuals with stereoanomalies show a diversity of deficits, which might be related to their individual clinical history. Recently tough, such asymmetry was reported also in an electrophysiological study in the normal cat visual cortex. Howarth, Vorobyov, and Sengpiel (2008) observed interocular transfer for monocular or near-monocular cells when the adapting stimulus was shown to the non-dominant eye, which in itself elicited little or no response. They found the strength of interocular transfer not to be linked to cell type, cortical layer, or location of recording sites within the cortical ocular dominance map. In the light of these findings Howarth et al. (2008) interpret interocular transfer as a reflection of interocular *modulatory* interaction rather than conventional binocularity. However this study was performed in cats with normal visual development. It remains uncertain whether the observed interocular transfer for monocular cells would be present in visually impaired animals and how it would relate to binocularity in these animals.

4.5. Relation to other fMRI studies in amblyopia

In contrast to previous fMRI studies in amblyopia which compared monocular stimulation of the amblyopic and non-amblyopic eyes (Algaze, Roberts, Leguire, Schmalbrock, & Rogers, 2002; Barnes, Hess, Dumoulin, Achtman, & Pike, 2001; Li, Dumoulin, Mansouri, & Hess, 2007; Liu et al., 2004; Muckli et al., 2006), we compare here the neuronal interactions between the ocular subsystems. We can however draw a few limited comparisons with previous studies that focused on the question how well does the amblyopic eye stimulate the visual cortex (Liu et al., 2004; Muckli et al., 2006). If we look at the peak response (Fig. 3) we can see some reduced activation for the amblyopic subjects in V1 (pooled over both eyes) and extrastriate visual cortex as has been reported by others (Barnes et al., 2001; Li et al., 2007). However, reduction of peak responses in amblyopes goes along with extended responses (until 12 s instead of 10) indicating more individual variance in the response dynamics that might contribute to smoothing and dampening of signal response. The difference vanishes if the activation is averaged from the peak until the end of the response (8–10 s shown in bar plots). Neither in V1 nor in extrastriate cortex are reductions of activity observed for the amblyopes. This comparison is crude, however, as both eyes are averaged in these conditions. If we compare monocular stimulation of the amblyopic eye (MonC, MonA, Fig. 4D) to monocular stimulation of the dominant eye (MonC, MonA, Fig. 4C) within the same subjects we find surprisingly high activation in V1, EXD and EXV. The amblyopic eyes show more BOLD response in the late time window than the dominant-eye in the same group or the normal subjects on either left or right eye. This result would be in line with previous finding of our group that reported good activation in response to amblyopic eye stimulation (Muckli et al., 2006).

The method of interocular transfer of adaptation developed in this study might prove useful for the objective assessment of cortical binocularity in clinical populations (possibly evaluating the effect of recently reported success of treatment – for a review of treatment, see Levi & Li, 2009). However, the single subject data does not provide enough power for significant effects on every subject. Although most subjects confirmed the general tendency the effects are too weak to be used reliably as a diagnostic tool. Further improvements of the paradigm, as for example careful selection of the adapting spatial/temporal frequency or finer tuning of the adapting/testing times (possibly employing times in the millisecond range), might increase the size of the measured effects or make the method less time-consuming. In this context, a recent fMRI study (Mirzajani et al., 2006) investigated the interaction of spatial and temporal frequencies in modulating the overall cortical response showing that the strength of the fMRI signal in response to different temporal frequencies was maximum at 6 Hz for high spatial frequency (8 cpd), while it was maximum at 8 Hz for low spatial frequency (0.5 cpd).

5. Conclusions

We developed a technique that enabled us to measure the amount of cortical cross talk (interactions) between the monocular subsystems. We tested our procedure in a group of amblyopic subjects known to have deficiencies in their interocular processing that is necessary to allow normal binocular vision. As a baseline for cortical cross-talk we determined orientation-specific adaptation effects within one monocular cortical subsystem. Subsequently, we tested the inter-cortical transfer of orientation-specific monocular adaptation. This strategy assured us to acquire the interaction of a specified and well studied cortical subsystem tuned to respond to contours of certain orientation (i.e. complex cells at the level of V1). With this method, we found consistent effects of *monoptic* as well as *dichoptic* orientation-specific fMRI adaptation in area V1 and in extrastriate areas on the ventral and dorsal visual stream of normally-sighted human observers. Our results show that, as suggested by animal studies and by previous psychophysical studies, early visual areas in the human brain possess a substantial amount of orientation-selective binocular cells. Additionally, we showed that the effects of fMRI adaptation in amblyopic subjects with compromised stereopsis differ fundamentally from those of subjects with intact stereopsis. Amblyopic subjects show consistent *monoptic*, but no *dichoptic* adaptation in area V1 and in extrastriate cortical regions on the ventral and dorsal cortical pathway. These results suggest that the neural circuits involved in binocular function and stereopsis might also be involved in the interocular transfer of pattern adaptation. The measured adaptation effects are only small in amplitude and for the presented analysis they were averaged over the group. For clinical purposes it would be desirable to have a technique that is able to

determine individually the amount of loss of the inter-ocular cross talk. However, the effects are only small and measurements would need to be extended over many hours to acquire sufficient power for such purposes. Developing functional imaging methods suited for the investigation of cortical binocular integration in individual clinical subjects remains a desirable task for the future.

Acknowledgments

We thank Wolf Singer for support and Axel Kohler for invaluable help at several stages during this study. We are grateful to Hanna Mues for help with data analysis, to Doris Baldauf, Iris Bachert, Peggy Feige and Licia Cirina for the orthoptical testing and to all the participants in this study for their patience. The work was supported by grants from the German Research Foundation (DFG) to Ruxandra Sireteanu (SI 344/17-1,2,3). Author BC was supported by a Scatcherd fellowship from the Oxford University.

References

Algaze, A., Roberts, C., Leguire, L., Schmalbrock, P., & Rogers, G. (2002). Functional magnetic resonance imaging as a tool for investigating amblyopia in the human visual cortex: A pilot study. *Journal of AAPOS, 6*, 300–308.

Alink, A., Singer, W., & Muckli, L. (2008). Capture of auditory motion by vision is represented by an activation shift from auditory to visual motion cortex. *Journal of Neuroscience, 28*(11), 2690–2697.

Barnes, G. R., Hess, R. F., Dumoulin, S. O., Achtman, R. L., & Pike, G. B. (2001). The cortical deficit in humans with strabismic amblyopia. *Journal of Physiology, 533*, 281–297.

Blake, R. (1982). Binocular vision in normal and stereoblind individuals. *American Journal of Optometry and Physiological Optics, 59*, 969–975.

Blakemore, C., & Campbell, F. W. (1969). On the existence of neurons in the human visual system selectively sensitive to the orientation and size of retinal images. *Journal of Physiology – London, 203*, 237–260.

Boynton, G. M., & Finney, E. M. (2003). Orientation-specific adaptation in human visual cortex. *Journal of Neuroscience, 23*, 8781–8787.

Boynton, G. M., Engel, S. A., Glover, G. H., & Heeger, D. J. (1996). Linear systems analysis of functional magnetic resonance imaging in human V1. *Journal of Neuroscience, 16*, 4207–4221.

Choubey, B., Jurcoane, A., Muckli, L., & Sireteanu, R. (2009). On dichoptic stimulus presentation in functional magnetic resonance imaging experiments. *The Open Neuroimaging Journal, 3*, 18–26.

Fang, F., Murray, S. O., Kersten, D., & He, S. (2005). Orientation-tuned FMRI adaptation in human visual cortex. *Journal of Neurophysiology, 94*, 4188–4195.

Fiorentini, A., Sireteanu, R., & Spinelli, D. (1976). Lines and gratings: Different interocular after-effects. *Vision Research, 16*, 1303–1309.

Furmanski, C. S., & Engel, S. A. (2000). An oblique effect in human primary visual cortex. *Nature Neuroscience, 3*, 535–536.

Goebel, R., Muckli, L., Zanella, F. E., Singer, W., & Stoerig, P. (2001). Sustained extrastriate cortical activation without visual awareness revealed by fMRI studies of hemianopic patients. *Vision Research, 41*(10–11), 1459–1474.

Goebel, R., Khorram-Sefat, D., Muckli, L., Hacker, H., & Singer, W. (1998). The constructive nature of vision: Direct evidence from functional magnetic resonance imaging studies of apparent motion and motion imagery. *European Journal of Neuroscience, 10*, 1563–1573.

Grill-Spector, K., & Malach, R. (2001). FMRI-adaptation: A tool for studying the functional properties of human cortical neurons. *Acta Psychologica (Amsterdam), 107*, 293–321.

Grill-Spector, K., Henson, R., & Martin, A. (2006). Repetition and the brain: Neural models of stimulus-specific effects. *Trends in Cognitive Sciences, 10*, 4–23.

von Grünau, M. W. (1982). Comparison of the effects of induced strabismus on binocularity in area 17 and the LS area in the cat. *Brain Research, 246*(2), 325–439.

Hamasaki, D. I., & Flynn, J. T. (1981). Amblyopic eyes have longer reaction times. *Investigative Ophthalmology and Visual Science, 21*, 846–853.

Hansen, B. C., & Essock, E. A. (2004). A horizontal bias in human visual processing of orientation and its correspondence to the structural components of natural scenes. *Journal of Vision, 4*, 1044–1060.

Hess, R. (1978). Interocular transfer in individuals with strabismic amblyopia: A cautionary note. *Perception, 7*, 201–205.

Hess, R. F., Hutchinson, C. V., Legdeway, T., & Mansouri, B. (2007). Binocular influences on global motion processing in the human visual system. *Vision Research, 47*, 1682–1692.

Hohmann, A., & Creutzfeldt, O. D. (1975). Squint and the development of binocularity in humans. *Nature, 254*, 613–614.

Howarth, C. M., Vorobyov, V., & Sengpiel, F. (2008). Interocular Transfer of Adaptation in the Primary Visual Cortex. *Cereb Cortex*. doi:10.1093/cercor/bhn211 (Epub ahead of print).

Hubel, D. H., & Livingstone, M. S. (1987). Segregation of form, color and stereopsis in primate area 18. *Journal of Neuroscience, 7*, 3378–3415.

Hubel, D. H., Wiesel, T. N., & LeVay, S. (1977). Plasticity of ocular dominance columns in monkey striate cortex. *Philosophical Transactions of the Royal Society of London Series B – Biological Sciences, 278*, 377–409.

Jurcoane, A., Choubey, B., Muckli, L., & Sireteanu, R. (2007). A pilot study for investigating amblyopia in the human visual cortex using functional magnetic resonance imaging. *Strabismus, 15*, 33–37.

Jurcoane, A., Mitsieva, D., Choubey, B., Muckli, L., & Sireteanu, R. (2008). Interocular transfer of fMRI adaptation in stereodeficient observers [Abstract]. *Journal of Vision, 8*(6), 97. doi:10.1167/8.6.97. <http://journalofvision.org/8/6/97/>.

Keck, M. J., & Price, R. L. (1982). Interocular transfer of the motion aftereffect in strabismus. *Vision Research, 22*(1), 55–60.

Kiorpes, L., & McKee, S. P. (1999). Neural mechanisms underlying amblyopia. *Current Opinion in Neurobiology, 9*, 480–486.

Kiorpes, L., Kiper, D. C., O'Keefe, L. P., Cavanaugh, J. R., & Movshon, J. A. (1998). Neuronal correlates of amblyopia in the visual cortex of macaque monkeys with experimental strabismus and anisometropia. *Journal of Neuroscience, 18*, 6411–6424.

Kourtzi, Z., & Kanwisher, N. (2001). Representation of perceived object shape by the human lateral occipital complex. *Science, 293*, 1506–1509.

Krekelberg, B., Boynton, G. M., & van Wezel, R. J. A. (2006). Adaptation: From single cells to BOLD signals. *Trends in Neurosciences, 29*, 250–256.

Larsson, J., Landy, M. S., & Heeger, D. J. (2006). Orientation-selective adaptation to first- and second-order patterns in human visual cortex. *Journal of Neurophysiology, 95*, 862–881.

Lerner, Y., Pianka, P., Azmon, B., Leiba, H., Stolovitch, C., Loewenstein, A., et al. (2003). Area-specific amblyopic effects in human occipitotemporal object representations. *Neuron, 40*(5), 1023–1029.

Levi, D. M., Klein, S. A., & Chen, I. (2008). What limits performance in the amblyopic visual system: Seeing signals in noise with an amblyopic brain. *Journal of Vision, 8*(4), 1–23.

Levi, D. M., & Li, R. W. (2009). Perceptual learning as a potential treatment for amblyopia: A mini-review. *Vision Research* (Epub ahead of print).

Li, X., Dumoulin, S. O., Mansouri, B., & Hess, R. F. (2007). Cortical deficits in human amblyopia: their regional distribution and their relationship to the contrast detection deficit. *Investigative Ophthalmology and Visual Science, 48*(4), 1575–1591.

Liu, GT., Miki, A., Francis, E., Quinn, G. E., Modestino, E. J., Bonhomme, G. R., et al. (2004). Eye dominance in visual cortex in amblyopia using functional magnetic resonance imaging. *Journal of AAPOS, 8*(2), 184–186.

Maffei, L., Fiorentini, A., & Bisti, S. (1973). Neural correlate of perceptual adaptation to gratings. *Science, 182*, 1036–1038.

Maraini, G., & Porta, R. (1978). Interocular transfer of a visual aftereffect in early-onset esotropia. *Archives of Ophthalmology, 96*, 1853–1856.

McColl, S. L., & Mitchell, D. E. (1998). Stereodeficient subjects show substantial differences in interocular transfer of two motion adaptation aftereffects. *Vision Research, 38*(12), 1889–1900.

McColl, S. L., Ziegler, L., & Hess, R. F. (2000). Stereo deficient subjects demonstrate non-linear stereopsis. *Vision Research, 40*(9), 1167–1177.

Meienbrock, A., Naumer, M. J., Doehrmann, O., Singer, W., & Muckli, L. (2007). Retinotopic effects during spatial audio-visual integration. *Neuropsychologia, 45*(3), 531–539.

Mitchell, D. E., & Ware, C. (1974). Interocular transfer of a visual after-effect in normal and stereoblind humans. *Journal of Physiology, 236*, 707–721.

Mirzajani, A., Oghabian, M. A., Riyahi-Alam, N., Saberi, H., Firouznia, K., & Bakhtiary, M. (2006). Spatial frequency modulates the human visual cortical response to temporal frequency variation: An fMRI study. *Conference Proceedings – IEEE Engineering in Medical and Biology Society, 1*, 1032–1035.

Mohn, G., & van Hof-van Duin, J. (1983). On the relation of stereoacuity to interocular transfer of the motion and the tilt aftereffects. *Vision Research, 23*(10), 1087–1096.

Movshon, J. A., & Lennie, P. (1979). Pattern selective adaptation in striate cortical neurones. *Nature, 278*, 850–852.

Movshon, J. A., Chambers, B. E. I., & Blakemore, C. (1972). Interocular transfer in normal humans, and those who lack stereopsis. *Perception, 1*, 483–490.

Movshon, T., & Newsome, W. T. (1996). Visual response properties of striate cortical neurons projecting to area MT in macaque monkeys. *Journal of Neuroscience, 16*, 7733–7741.

Muckli, L., Kieß, S., Tonhausen, N., Singer, W., Goebel, R., & Sireteanu, R. (2006). Cerebral correlates of impaired grating perception in individual, psychophysically assessed human amblyopes. *Vision Research, 46*, 506–526.

Muckli, L., Kohler, A., Kriegeskorte, N., & Singer, W. (2005). Primary visual cortex activity along the apparent-motion trace reflects illusory perception. *PLoS Biology, 3*(8), e265–e275.

Murray, S. O. (2008). The effects of spatial attention in early human visual cortex are stimulus independent. *Journal of Vision, 8*(10), 2.1–2.11.

Neri, P. (2005). A stereoscopic look at visual cortex. *Journal of Neurophysiology, 93*, 1823–1826.

Popple, A. V., & Levi, D. M. (2008). The attentional blink in amblyopia. *Journal of Vision, 31*(8(13)), 12.1-9.

Raymond, J. E. (1993). Complete interocular transfer of motion adaptation effects on motion coherence thresholds. *Vision Research, 33*, 1865–1870.

Rice, M. L., Leske, D. A., Smestad, C. E., Holmes, J. M. (in press). Results of ocular dominance testing depend on assessment method. *Journal of AAPOS*. doi:10.1016/j.jaapos.2008.01.017.

Schröder, J., Fries, P., Roelfsema, P. R., Singer, W., & Engel, A. K. (2002). Ocular dominance in extrastriate cortex of strabismic amblyopic cats. *Vision Research, 42*, 29–39.

Seijas, O., Gómez de Liaño, P., Gómez de Liaño, R., Roberts, C. J., Piedrahita, E., & Diaz, E. (2007). Ocular dominance diagnosis and its influence in monovision. *American Journal of Ophthalmology, 144*(2), 209–216.

Shipp, S., & Zeki, S. (1989). The organization of connections between areas V5 and V1 in macaque monkey visual cortex. *European Journal of Neuroscience, 1*, 309–332.

Simola, J., Stenbacka, L., & Vanni, S. (2009). Topography of attention in the primary visual cortex. *European Journal of Neuroscience, 29*(1), 188–196.

Sireteanu, R., & Best, J. (1992). Squint-induced modification of visual receptive fields in the lateral suprasylvian cortex of the cat: Binocular interaction, vertical effect and anomalous correspondence. *European Journal of Neuroscience, 4*, 235–242.

Sireteanu, R. (1991). Restricted visual fields in both eyes of kittens raised with a unilateral, surgically induced strabismus: Relationship to extrastriate cortical binocularity. *Clinical Vision Sciences, 6*, 277–287.

Sireteanu, R., Fronius, M., & Singer, W. (1981). Binocular interaction in the peripheral visual field of humans with strabismic and anisometropic amblyopia. *Vision Research, 21*, 1065–1074.

Somers, D. C., Dale, A. M., Seiffert, A. E., & Tootell, R. B. (1999). Functional MRI reveals spatially specific attentional modulation in human primary visual cortex. *Proceedings of the National Academy of Sciences of the United States of America, 96*, 1663–1668.

Talairach, J., & Tournoux, P. (1988). *Co-planar stereotaxic atlas of the human brain*. New York: Thieme Medical Publisher Inc.

Vanni, S., Henriksson, L., & James, A. C. (2005). Multifocal fMRI mapping of visual cortical areas. *Neuroimage, 27*(1), 95–105.

Wade, N. J. (1976). On interocular transfer of the movement after-effect in individual with and without normal binocular vision. *Perception, 5*, 113–118.

Ware, C., & Mitchell, D. E. (1974). On interocular transfer of various visual after-effects in normal and stereoblind observers. *Vision Research, 14*, 731–734.

Webber, A. L., Wood, J. M., Gole, G. A., & Brown, B. (2008). The effect of amblyopia on fine motor skills in children. *Investigative Ophthalmology and Visual Science, 49*(2), 594–603.

Weigelt, S., Kourtzi, Z., Kohler, A., Singer, W., & Muckli, L. (2007). The cortical representation of objects rotating in depth. *Journal of Neuroscience, 27*, 3864–3874.

Weigelt, S., Muckli, L., & Kohler, A. (2008). Functional magnetic resonance adaptation in visual neuroscience. *Reviews in the Neuroscience, 19*(4-5), 363–380.

Wolfe, J. M., & Blake, R. (1985). Dissecting the binocular visual system with psychophysical tools. In D. Rose & V. G. Dobson (Eds.), *Models of visual cortex* (pp. 192–199). New York: Wiley & Sons.